Sixteenth Quarterly Progress Report

May 1, 2010 to July 31, 2010
Contract No. HHS-N-260-2006-00005-C
Neurophysiological Studies of Electrical Stimulation for the Vestibular Nerve

Submitted by:
James O. Phillips, Ph.D.[1,3,4]
Steven Bierer, Ph.D. [1,3,4]
Albert F. Fuchs, Ph.D. [2,3,4]
Chris R.S. Kaneko, Ph.D. [2,3]
Leo Ling, Ph.D. [2,3]
Shawn Newlands, M.D., Ph.D. [5]
Kaibao Nie, Ph.D. [1,4]
Jay T. Rubinstein, M.D., Ph.D. [1,4,6]

[1] Department of Otolaryngology-HNS, University of Washington, Seattle, Washington
[2] Department of Physiology and Biophysics, University of Washington, Seattle, Washington
[3] Washington National Primate Research Center, University of Washington, Seattle, Washington
[4] Virginia Merrill Bloedel Hearing Research Center, University of Washington, Seattle, Washington
[5]Department of Otolaryngology, University of Rochester, Rochester, New York
[6] Department of Bioengineering, University of Washington, Seattle, Washington

Reporting Period: May 1, 2010 to July 31, 2010

Challenges: Our main challenge for this quarter has been in adapting our software to provide real time frequency modulated inputs at a fixed minimal latency. We have been able to complete programming using SDK for a real time frequency modulated electrical stimulus. This is an important accomplishment and it is described in our current successes below. However, there are significant limitations to this system that we do not fully understand at this time. The main limitation is that the device, when triggered by a 5 volt square wave input, produces a step in frequency with a lag of 60.4 ms, and then when the same square wave steps back, with a negative voltage step, there is a step in frequency with a lag of 14.6 ms. This is shown in Figure 1.

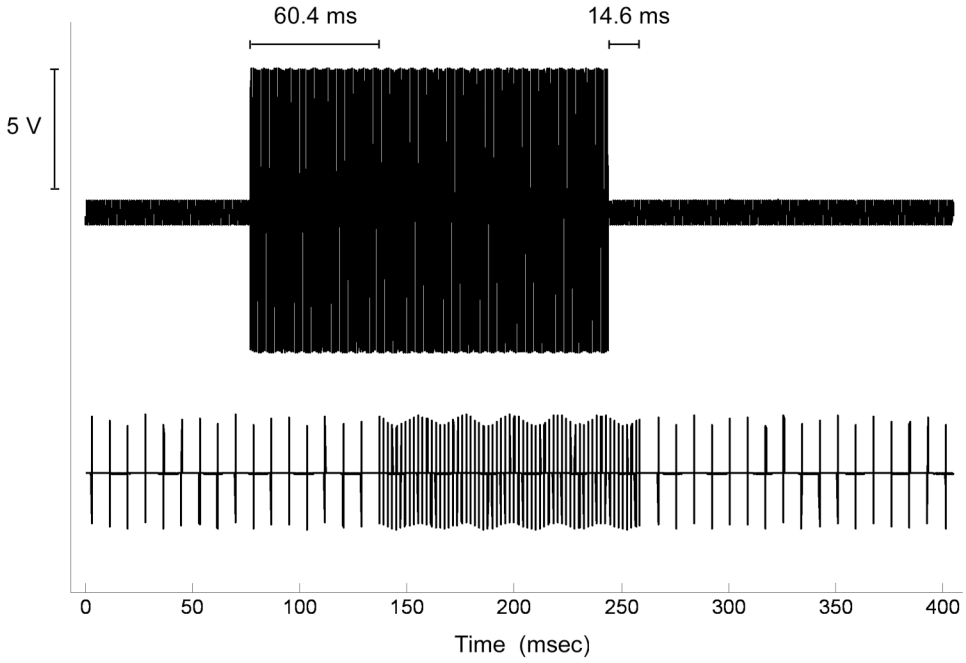

Figure 1. A brief 100 ms stimulus train triggered by a voltage step using the new SDK real time FM processing. The upper trace shows the voltage step used to drive the electrical stimulus train. The lower trace shows the output of an implant in a box during a bench test.

This result could be due to the impedance of the input source, and it does not affect application of the device as a pacemaker to treat intermittent vertigo. However, it does mean that the device is not ready for prime time as a real time vestibular prosthesis. We must be able to produce much shorter and consistent response delays to make a device that can respond to high frequency head velocity stimuli with a minimal phase delay. Otherwise, the device will be of limited utility during high frequency head rotations, which are within the natural frequency of human head movements.

Our response to this challenge has been to shift additional resources to the programming, bench testing, and recording in vivo of short stimulation trains that are generated by the device running in the SDK environment.

Successes: We have made significant strides in several areas as noted below.

1. We have recorded vestibular stimulation responses during natural head unrestrained gaze shifts in two animals. The objective of this study is two fold. First, we are trying to understand the interaction between normal gaze shifts, in which the vestibular input must be precisely modulated, and electrically supplemented vestibular input. We want to know how the vestibular system deals with this signal, and if it is treated as a normal head velocity signal. Second, we are interested in discovering the timing of the changes in vestibulo-ocular reflex (VOR) gain that accompany head unrestrained gaze shifts. We are using this stimulus as a well controlled perturbation to the head velocity input to ongoing gaze movements.

Our approach is conceptually straightforward. We trained two monkeys to make head unrestrained gaze shifts, and head fixed saccades, for an applesauce reward. Then we developed a strategy for delivering conditionally triggered short (50 to 100 ms duration) constant frequency stimulation trains. We recorded eye velocity responses to short trains of different stimulation frequencies and currents in each animal generated with the NIC 2 processor. We then reproduced the same data using the clinical processor driven in real time and triggered by an eye velocity threshold or a target step. The control data was obtained in the dark following head fixed saccades, at a time when the literature suggests that the VOR gain should be essentially 1.0. We then compared the eye movement velocities recorded under these conditions with the eye movement velocities recorded when the stimulation occurred at different times during a head unrestrained gaze shift.

Despite its conceptual simplicity, this project required considerable investment in developing the tools required and making the actual measurements. These tools are a valuable asset to our laboratory and will be used extensively in our experiments in year 5.

First, we had to configure the Cochlear Freedom clinical interface to trigger pulse trains in real time. The head-unrestrained and head-restrained gaze perturbation experiments required accurate and precise timing of the electrical stimuli. The "VI Stream" software that our lab usually uses to deliver vestibular implant stimulation is not suitable for this purpose because of the inherent delays in triggering the Cochlear NIC-2 research interface. For this reason, we used the standard clinical processor, appropriating the audio input channel to control the timing and amplitude of the pulse train output. The approach is similar to that described in QPR 11 for real-time amplitude modulation, with a few important differences.

Triggering set-up. The analog input signal to the implant processor was a 1 kHz zero-mean square wave delivered by a Nuclear-Chicago stimulator, which took the place of the 1 kHz sinusoidal carrier waveform used in the AM experiments. The voltage amplitude of the square wave was manually set (over the range 0 – 6 V), providing

convenient control over the amplitude of the final output pulses. The Nuclear-Chicago stimulator was triggered by a Spike2 data acquisition system, based on a user-set eye velocity threshold or timed to the visual target. The square wave duration was typically set to 50 or 100 ms. The resulting "on-or-off" square wave signal, connected to the auxiliary input jack of the clinical processor, was used to trigger pulse trains according to the processor's mapping configuration.

Processor set-up. The clinical processor was programmed using the Custom Sound 2.0 clinical mapping software. The channel of stimulation, pulse width, and pulse rate (limited by the software to 250 or 500 pps) were set according to the requirements of the experiment. Current threshold was defined as 0 CL (clinical level) and maximum current was set to the highest level without stimulating the facial nerve, based on observations using VIStream. As described in QPR 11, the input-output function was made as linear as possible, using a "Q" value of 50. To reduce microphone pickup, the microphone gain was set to the lowest allowable value and the microphone ear-piece was enclosed in foam to further attenuate acoustic noise.

Because the input signal from the Nuclear-Chicago is a square wave, it contains spectral energy outside of the 1 kHz fundamental frequency. Bench-top tests indicated that if the analytical bandpass filter for the stimulation channel was too wide, energy in the higher harmonics could cause the output pulses to fluctuate in current level (at a rate of several Hz) for a constant input amplitude. This non-stationarity is likely a product of the fast-Fourier transform algorithm implemented by the processor. Therefore, to prevent fluctuations, we set the bandpass range to 750 - 1250 Hz to eliminate the higher harmonics.

Timing calibration. Calibrations were performed using an "implant-in-a-box", with the output channel connected to ground via a 10 kOhm resistor to convert electrical current to voltage. Figure 2 shows an example of a square wave input waveform and the resulting pulse train delivered to the vestibular implant. The top trace is the trigger signal, which in an actual experiment would be timed to a saccade or target shift. The square wave from the Nuclear Chicago stimulator, in the middle trace, starts immediately at the 0 to 5 V rise of the trigger signal. The duration of the square wave in this example was manually set to ~44 ms. The final pulse train output, delivered to channel 6 of the implant, is displayed in the bottom trace. The attributes of the pulse train reflect how the processor was programmed, with a pulse rate of 500 pps and a pulse width of 100 μs/phase. The train is ~44 ms in duration, matching the duration of the analog input. Because of processing delays, the pulse train lags the input waveform by 13.6 ms. Additionally, the first and last pulse are smaller than the middle pulses, because the spectral energy of the square wave input is measured over discrete time windows. (The slight jitter in amplitude during the sustained portion of the pulse train is a result of undersampling by the data acquisition system.)

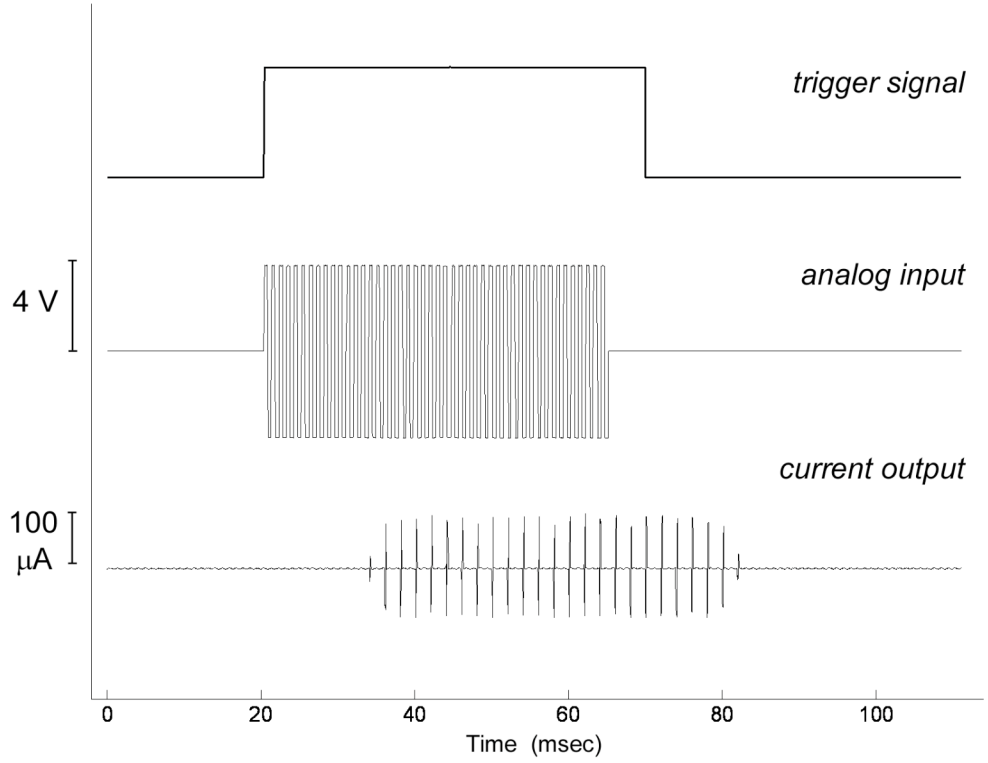

Figure 2. Triggered stimulation of the clinical processor, as used in the gaze perturbation experiments. From top to bottom, the signals represent the 5V trigger to the Nuclear-Chicago stimulator, the square wave analog output of the Nuclear-Chicago, and the resulting train of current pulses from one implant channel (delivered through the "implant-in-a-box" processor).

Across repeated presentations of 500 pps pulse trains, the average first-pulse latency with respect to the square wave input was 14.1 ms, with a range of 12.5 to 15.7 ms. Thus, the timing accuracy of the clinical processor is much faster than the latency we typically observe with the research interface and VIStream (NIC-2) software, which is approximately 200 ms. While latencies near 15 ms are acceptable for the gaze perturbation experiments, a shorter latency is desirable for eliciting VOR responses to head motion in real time. Ultimately a vestibular prosthesis system will not require the audio processing components that are useful for cochlear implants, such as automatic gain control and bandpass filtering, and can therefore have a shorter overall processing delay.

Amplitude calibration. An example calibration of the pulse train currents, with respect to the voltage amplitude of the Nuclear-Chicago square wave signal, is shown in Figure 3. The threshold and "most-comfortable" current levels were set in the Custom Sound software at 0 and 120 CL, respectively. Also, the manual volume control on the audio cable was at "2", and the volume and sensitivity processor settings were at 9 and 0, respectively. As seen in the figure, the voltage-to-current calibration is approximately linear after an initial jump to ~20 μA, which is the minimum allowable current step for

the Freedom processor. The function saturates at 6 volts at a current of 165 μA, corresponding to the maximum comfort level.

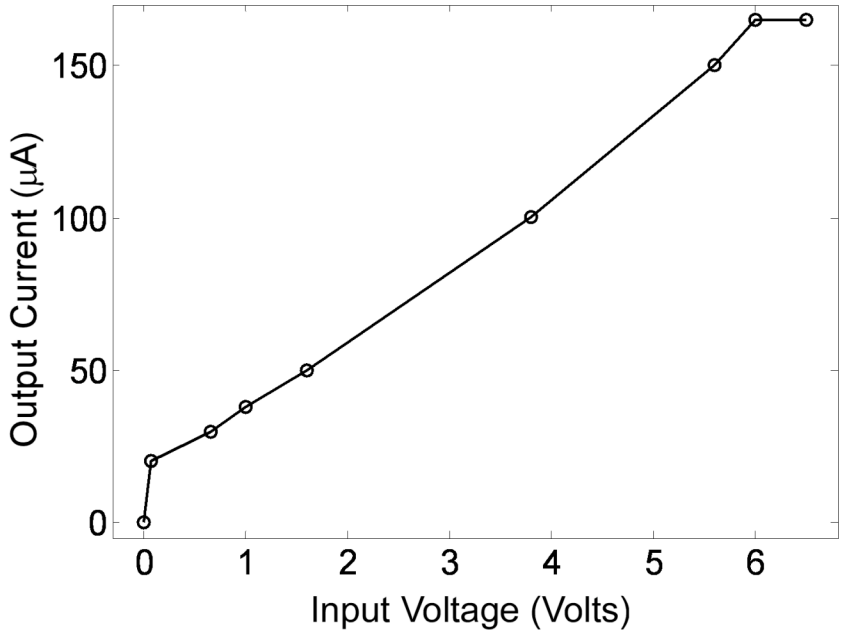

Figure 3. Calibration of pulse train current with respect to the voltage amplitude of the square wave input signal

Gaze perturbation. The general result of our eye velocity triggered short duration stimulus train perturbation of head unrestrained gaze shifts is shown in Figure 4. Stimuli were monopolar with a 100 μs pulse width and a stimulation rate of 500 pps. The stimuli were triggered at a latency of 100 ms from a settable eye velocity limit. The duration of stimulation was 50 ms. The eye velocity that resulted from short duration stimulation was in the plane of the implanted canal, which was co-planar to the direction of the target step and the elicited gaze shift; either in the direction of the gaze shift or in the direction opposite to the direction of the gaze shift. Stimulation immediately following a saccade elicited a consistent change in eye velocity that was equal to or greater than the change in gaze velocity that resulted from stimulation during the gaze shift. The resulting change in gaze velocity had the expected latency of 10 ms (24 ms following the onset of the stimulus command), which is consistent with the literature. The magnitude of the velocity transient was somewhat greater for gaze shifts directed toward the stimulated ear than for those directed away from the stimulated ear. One interesting feature of the eye velocity change during the gaze shift, that was different from that following a saccade, was that there was a compensatory reduction in eye velocity following a stimulation elicited eye velocity increase, and a similar compensatory increase in eye velocity following a stimulation elicited eye velocity decrease. Such compensation has been observed during torque pulse perturbation of gaze shifts, and is therefore consistent with normal processing of head velocity information.

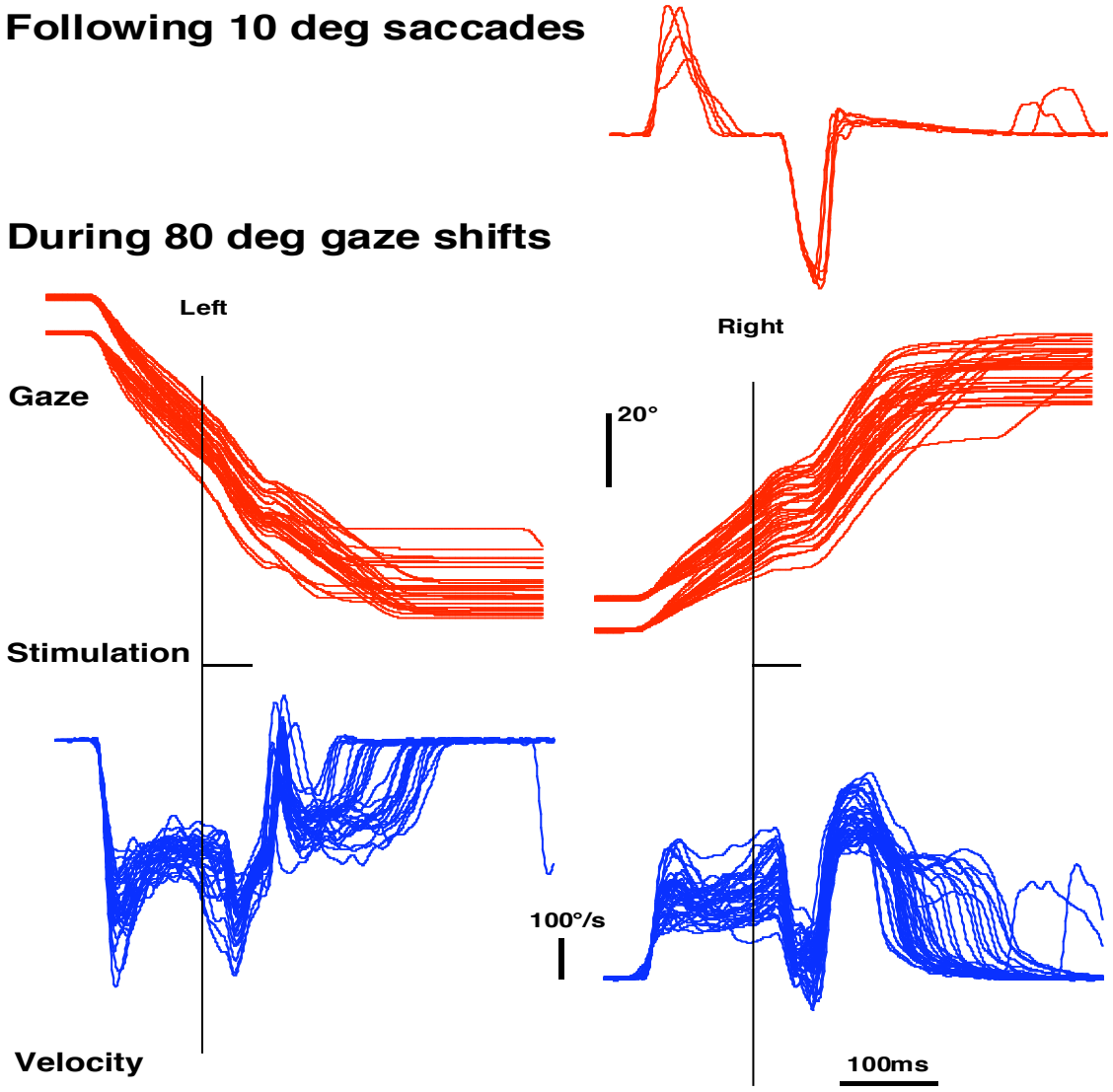

Figure 4: Electrical stimulation during gaze shifts and following saccades. Gaze velocity showed appropriate acceleration and deceleration during gaze shifts.

Since increasing stimulation current produces increasing slow phase velocity, we looked to see the result of increasing the current intensity of the 50 ms electrical stimulus perturbing rightward directed 60 deg gaze shifts. The results are illustrated in Figure 5. Increasing stimulation current produced increased velocity perturbations in the gaze trajectory, suggesting that the increased current was interpreted as increased head velocity, and was used to modify the trajectory of the gaze movement. Furthermore, increasing stimulation current produced a decrease in the overall amplitude of the gaze movement. In Figure 5, although there is some overlap, there is a decrease in gaze amplitude for the red (150uA stimulation current) traces versus the green (100uA) traces, and the blue (125uA) traces fall in between. This suggests that the head velocity signals derived from the electrical stimulation were used to calculate gaze error during the head free gaze shift, as if they were from natural head movements.

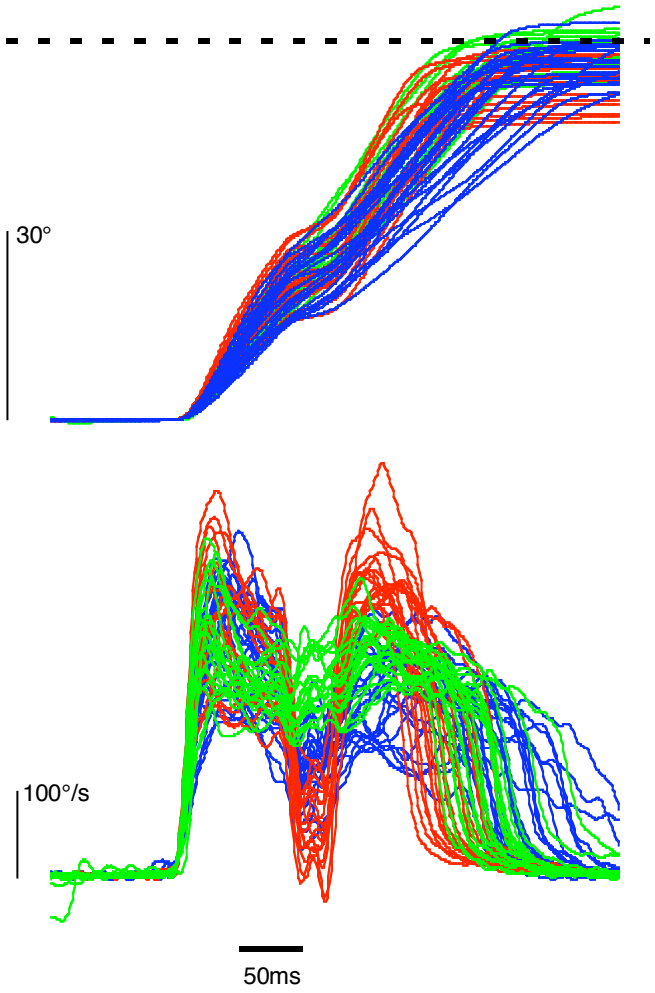

Figure 5: Result of electrical stimulation at different current intensities during head unrestrained gaze shifts to 60 deg target steps. Upper traces are gaze position, and lower traces are gaze velocity. Stimulation currents are 100, 125, 150 μA.

2. We have successfully implemented the real-time FM pulse train stimulator using the Nucleus SDK interface. All the issues that we encountered in our previous software development have been addressed after intensive investigations and software programming. The purpose of the real-time FM stimulator is to use amplitude-modulated (AM) analog signals to control frequency-modulated (FM) pulse trains in real-time. We were able to build a fully functional SDK firmware based on the exemplar modules provided by Cochlear Ltd. We created several software modules with assembly codes for the purpose of implementing the AM-to-FM transformation. The firmware running on a clinical Nucleus Freedom processor can take direct audio input and transform it in real-time into frequency-modulated pulse trains at a given range of pulse rate. For example, the slowly varying chair rotational signals can be used to amplitude modulate a carrier at 1000 Hz and then can be fed into the auxiliary audio input port on a Nucleus Freedom processor. The firmware that we built can detect the envelope of the amplitude-modulated signal and then determine the pulse rate of the FM trains. The envelope

extraction was implemented with a fast peak detector to avoid long latency with the traditional envelope detectors such as half-wave rectification followed by a low-pass filter. The lowest pulse rate can be as low as 10 pps in our current implementation and the highest rate can be up to several 1000 pps with no limitation. The real-time FM stimulator has been evaluated in one of our implanted monkeys.

We first tested the FM capabilities with the implant-in-a-box stimulator. The clinical processor was programmed using the SDK-enhanced mapping software. Channel 6 was configured in the monopolar mode to produce 100 μs/phase biphasic pulses at a fixed current of 100 μA and at pulse rates over the range 100 to 500 pps. The input signal, which was delivered through the audio jack of the clinical interface, was generated by mixing the output waveform of a function generator with a continuous 1 kHz sinusoid. The envelope and amplitude of the resulting amplitude-modulated waveform were manually adjustable. The output current of channel 6 was transduced as a voltage across a 10 kOhm resistor and, along with the input signal, recorded by the Spike2 data acquisition system.

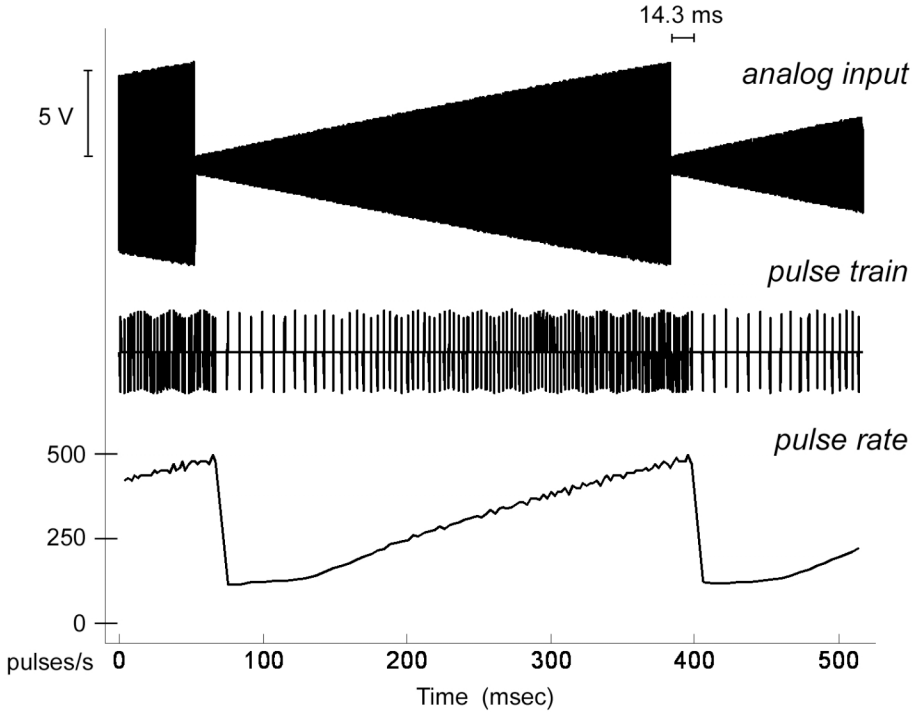

Figure 6. Example of a frequency modulated pulse train generated by a ramping analog input signal. The horizontal time bar at the top indicates the latency of the pulse train with respect to the input.

Slow sinusoidal modulation of the input between 0.4 and 6.1 volts produced the full range of frequency modulation at the output from 100 to 500 pps. The pulse rate also followed other types of input modulations, including square waves and ramps. An example of pulse rate changes during a full cycle of a positive-going ramp (at ~3

cycles/sec) is shown in Figure 6. As the input waveform increased in voltage, the pulse rate increased nearly linearly from 100 to 500 pps. Note that the timing of the abrupt drop in pulse rate at the end of the ramp cycle was delayed relative to the input waveform. As described previously, this latency, measured at 14.3 ms in this example, is the result of digital processing delays.

An example of eye movement responses to frequency modulated stimulation is shown in Figure 7. The modulating waveform at the input was a 0.5 Hz sinusoid transversing the full voltage range (~0.4 - 6.0 volts, calibrated at 100 – 500 pps), and an electrode in the lateral canal was chosen for monopolar stimulation at 100 μA. Two cycles of stimulation are displayed in the figure. As expected from previous experiments in our laboratory using sequenced FM pulse trains, slow phase horizontal eye velocity (depicted in the bottom trace with saccades displayed in light grey) was entirely leftward (negative) and modulated at 0.5 Hz.

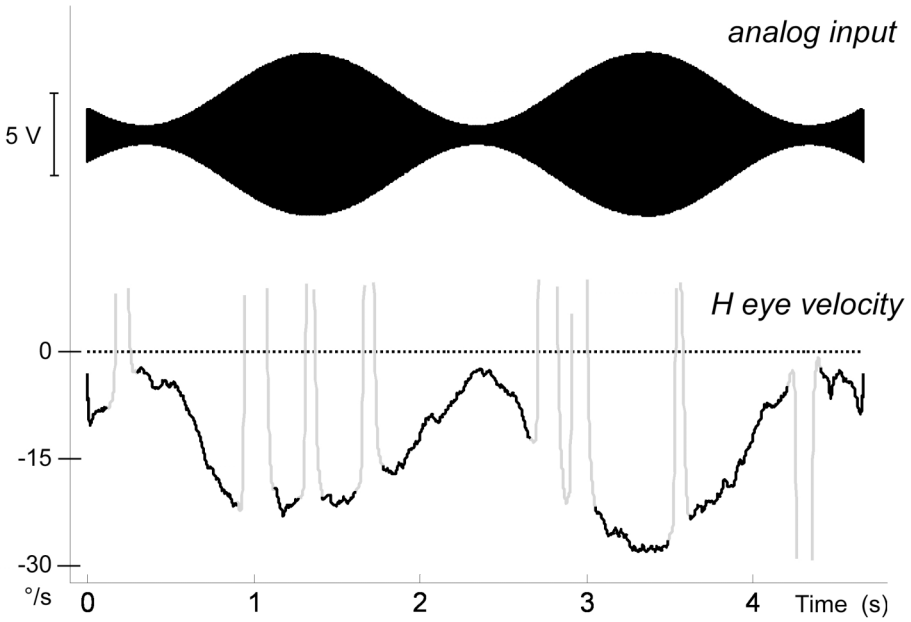

Figure 7. Example of modulated slow phase eye velocity generated by 0.5 Hz sinusoidal modulation of the pulse rate (calibrated to range between 100 and 500 pps as in Fig. 6). Current is fixed at 100 μA.

3. We have successfully implemented the customized maps and programs for the forthcoming human trials to treat Meniere's disease with our vestibular implant. The goal was to create constant-amplitude pulse trains on a specified electrode with the SDK interface and software to allow a subject to adjust the pulse amplitude between the threshold level and the most comfortable level by pushing the volume control button on a Nucleus Freedom speech processor. The subject can also switch between 3 different maps by pushing the power button. These functions all have been implemented and verified. We are ready to program the Nucleus Freedom processor with up to 3 customized maps that can produce the designed pulse trains.

4. We have successfully performed several multiple electrode stimulation summation experiments in 3 monkeys. We recorded slow phase eye velocities in response to trains of electrical canal stimulation, systematically varying either the current or the frequency of stimulation in one canal, while holding the stimulation in the other canal constant. A typical result is illustrated in Figure 8, which shows the result of constant frequency and current stimulation in a lateral canal electrode combined, briefly, with constant frequency stimulation of an electrode in the posterior canal at different current levels. The results show a summation of the eye velocities elicited by stimulation of each canal alone.

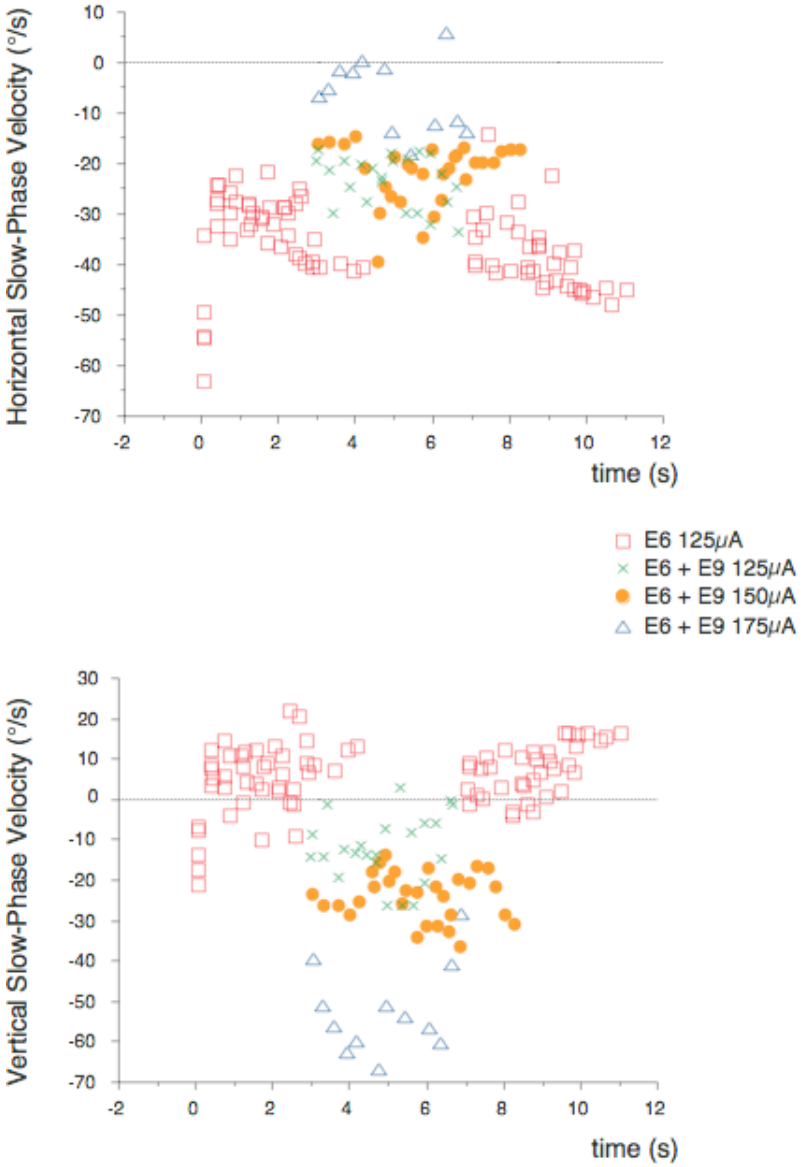

Figure 8. Summation of lateral (E6) and posterior canal (E9) electrical stimulation.

Stimulation of the right lateral canal alone produces slow phase velocities that are largely directed leftward and somewhat upward, presumably due to current spread to the anterior canal. Stimulation of the right posterior canal produces largely downward but also

rightward directed slow phase velocity. When the two stimuli are combined, with increasing posterior canal current, there is an increasing downward velocity and a decreasing leftward velocity, as predicted by velocity summation.

5. We have begun our experimental reconstruction of four monkey temporal bones and brains. This quarter we began histology on our past prosthesis specimens. The goal of these studies will be to visualize the placement of the vestibular stimulating device and assess the placement of the electrodes within the semicircular canals. We will look for aberrant tissue surrounding the electrode sites within the vestibular labyrinth, which may provide further indication of the biosafety of the device. In addition, we will perform histology on the brainstem to confirm locations of electrophysiological recordings.

At this time, we have completed experiments with several animals that have each had at least one vestibular implant. After behavioral and electrophysiological studies were completed, each animal was euthanized and immediately perfused with 10% Neutral Buffered Formalin (NBF), pH 6.8, to fix the tissue. The heads were then removed and stored in 10% NBF for future study. In two of the specimens, the brainstem was removed immediately after the perfusion and stored in 10% NBF.

With the intact specimens, we will use a series of CT scans to image the prosthesis and placement of the electrodes in situ. Once we have these images, we will then dissect out our areas of interest, which include the brainstem and the electrode-containing temporal bones. The temporal bones will be re-scanned in a micro-CT scanner for a higher resolution image of the specific electrode placement. Once we have the micro-CT images, the temporal bones will be embedded in celloidin, dehydrated, and decalcified in a process that allows us to look at the membranous labyrinth structures within the inner ear. Again, we will be interested in the electrode placement as well as the state of tissues surrounding the embedded electrodes. Finally, we will look at the brainstems of all of our specimens. These will be embedded in gelatin and then sliced using a cryomicrotome. These slices will then be mounted, stained, and examined to verify of the locations of the electrical recording sites.

6. We have presented three abstracts at international and national scientific meetings.

Nie, K., Bierer, S., Ling, L., Oxford, T., Phillips, J., Rubinstein, J. *Characterization of the Electrically-Evoked Compound Action Potential of the Vestibular Nerve.* American Otologic Society, Las Vegas, NV. 2010

Phillips, J., Ling, L., Fuchs, A., Kaneko, C.R.S., Bierer, S., Nie, K., Oxford, T. Newlands, S., Rubinstein, J. *Evaluation of a chronically implanted prosthesis to parametrically control nystagmic eye movements.* Association for Research in Vision and Ophthalmology, #4761, Ft. Lauderdale, FL 2010

Steven M. Bierer, Leo Ling, Kaibao Nie, Albert Fuchs, Trey Oxford, Chris Kaneko, Jay T. Rubinstein, and James O. Phillips *Behavioral results from an implantable vestibular*

prosthesis based on commercial cochlear implant technology., Neural Interfaces Conference, Long Beach, CA, 2010

7. We have presented two invited lectures.

Jay T. Rubinstein, Bionic Ear Institute, University of Melbourne, "*Roadmap to a human vestibular implant"*,7/28/2010

Jay T. Rubinstein, Frontiers in Otolaryngology, Garnet Passe and Rodney Williams Foundation, Melbourne, Australia, *"Roadmap to a human vestibular implant"*, 7/29/2010

8. We completed two papers for presentation and subsequent publication in Quarter 17. The papers were presented at the 2010 Barany Pre-Meeting, The Vestibular System: Current Research and Future Directions (A Congress in Honour of Jay Goldberg) in Reykholt, Iceland and the Barany 2010 Main Meeting in Reykjavik Iceland in Quarter 17.

Phillips, J., Ling, L., Fuchs, A., Kaneko, C.R.S., Bierer, S., Nie, K., Oxford, T. Newlands, S., Rubinstein, J. *Discharge frequency versus recruitment coding for a unilateral vestibular implant.*

Fuchs, A.F., Ling, L., Newlands, S. and Phillips, J. *Signals Carried by the Brainstem Saccade Generator in Semicircular Canal Plugged Monkeys: Implications for the Control of Gaze*.

9. We have received WIRB approval for a human clinical trial of our vestibular implant. We anticipate beginning a human clinical trial in Quarter 17.

Objectives for Quarter 17.

1. In next quarter, we will continue our software development on the SDK platform. We will work to produce consistent minimal delays between the amplitude modulated input command signal and the frequency modulated electrical output of the device.

2. We will initiate our human clinical study of the safety and efficacy of the vestibular prosthesis for the treatment of Meniere's disease in human subjects.

3. We will continue single unit recording studies with the objective of understanding the precise mechanism that allows for summation of natural and electrical stimuli during head unrestrained gaze shifts. We plan to record from neurons that respond with burst or pause discharge during head unrestrained gaze shifts, both in the vestibular nuclei and in the pontine brainstem, and electrically stimulate the vestibular end organ during the burst. This will tell us if these elements are processing vestibular signals during head unrestrained gaze shifts. This will address a current controversy in the literature, and provide more information about the natural combination of active movements and electrically elicited head velocity signals.

4. We will continue our ongoing behavioral testing by further recording behavioral responses to parametrically controlled summation of stimulation from two canals, and bipolar stimulation between canals.

5. We will continue our histological studies of temporal bones and the brainstem location of recorded neurons.